Adsorption of Benzene on Graphitized Thermal Carbon Black: Reduction of the Quadrupole Moment in the Adsorbed Phase

D. D. Do* and H. D. Do

Department of Chemical Engineering, University of Queensland, St. Lucia, Qld 4072, Australia

Received September 18, 2005. In Final Form: November 28, 2005

The performance of intermolecular potential models on the adsorption of benzene on graphitized thermal carbon black at various temperatures is investigated. Two models contain only dispersive sites, whereas the other two models account explicitly for the dispersive and electrostatic sites. Using numerous data in the literature on benzene adsorption on graphitized thermal carbon black at various temperatures, we have found that the effect of surface mediation on interaction between adsorbed benzene molecules must be accounted for to describe correctly the adsorption isotherm as well as the isosteric heat. Among the two models with partial charges tested, the WSKS model of Wick et al.[1] that has only six dispersive sites and three discrete partial charges is better than the very expensive all-atom model of Jorgensen and Severance.[2] Adsorbed benzene molecules on graphitized thermal carbon black have a complex orientation with respect to distance from the surface and also with respect to loading. At low loadings, they adopt the parallel configuration relative to the graphene surface, whereas at higher loadings (still less than monolayer coverage) some molecules adopt a slant orientation to maximize the fluid−fluid interaction. For loadings in the multilayer region, the orientation of molecules in the first layer is influenced by the presence of molecules in the second layer. The data that are used in this article come from the work of Isirikyan and Kiselev,[3] Pierotti and Smallwood,[4] Pierce and Ewing,[5] Belyakova, Kiselev, and Kovaleva,[6] and Carrott et al.[7]

1. Introduction

The adsorption of gases or vapors on solid surfaces such as graphitized thermal carbon black (GTCB) has been extensively studied in the literature[8−16] because such a material if graphitized adequately can yield a very homogeneous surface.[17−18] This material is, therefore, often used as a reference material for the characterization of the interaction between a molecule and surface carbon atoms. It must be noted, however, that such a surface of highly graphitized thermal carbon black is not necessarily the same as the surface of porous carbon material because the latter is most likely to be heterogeneous because of defects and the presence of functional groups.

The adsorption of simple gases, such as noble gases, and lower-order hydrocarbons on GTCB has been substantially studied in the literature.[8] However, for hydrocarbons such as aromatics (benzene and the like) work has been limited, especially the comparison between GCMC simulation results of benzene adsorption on graphitized thermal carbon black and experimental data. In particular, the performance of various intermolecular potential models in the description of data has not been carried out in the literature. Furthermore, it is known that benzene has a strong intermolecular interaction in the bulk phase, and if that is unchanged during adsorption on surfaces, it is expected that such a strong cohesive force could give S-shaped adsorption isotherms on surfaces such as graphite. However, experimental data shows no such S shape for benzene adsorption at ambient temperature.[3,4] It is therefore the objective of this article to study systematically the adsorption of benzene on the carbon black surface by using the grand canonical Monte Carlo (GCMC) simulation method.[19−21] The physical properties of benzene are listed in Table 1. (For comparison, we also list the properties of carbon dioxide in the same Table.)

Table 1. Properties of Benzene and Carbon Dioxide

		benzene	carbon dioxide
T_c	K	562.1	304.2
P_c	Pa	4.894×10^6	7.376×10^6
V_c	m^3/kmol	0.259	0.094
T_b	K	353.3	194.7
T_{tr}	K	278.7	216.6
P_{tr}	Pa	4.785×10^3	5.736×10^5
quadrupole moment	C m^2	-23.9×10^{-40}	-14.9×10^{-40}
dipole	D	0	0

2. Theory

To simulate the adsorption isotherms we use the grand canonical Monte Carlo simulation, first proposed by Norman and Filinov.[19] This simulation technique is described in detail in a number of books.[20,21]

Multisite Potential Model. Because of the flat hexagonal shape of benzene, it should not be treated as a single interaction site particle because in the confined space of pores the molecular

* Corresponding author. E-mail: duongd@cheque.uq.edu.au. Phone: +61-7-3365-4154. Fax: +61-7-3365-2789.

(1) Wick, C. D.; Siepmann, J. I.; Klotz, W. L.; Schure, M. R. *J. Chromatogr., A* **2002**, *954*, 181.
(2) Jorgensen, W. L.; Severance, D. L. *J. Am. Chem. Soc*. **1990**, *112*, 4768.
(3) Isirikyan, A. A.; Kiselev, A. V. *J. Phys. Chem.* **1961**, *65*, 601.
(4) Pierotti, R. A.; Smallwood, R. E. *J. Colloid Interface Sci.* **1966**, *22*, 469.
(5) Pierce, C.; Ewing, B. *J. Phys. Chem.* **1967**, *71*, 3408.
(6) Belyakova, L. D.; Kiselev, A. V.; Kovaleva, N. V. *Russ. J. Phys. Chem.* **1968**, *42*, 1204.
(7) Carrott, P. J. M.; Ribeiro Carrott, M. M. L.; Cansado, I. P. P.; Nabais, J. M. V. *Carbon* **2000**, *38*, 465.
(8) Avgul, N.; Kiselev, A. V. *Chem. Phys. Carbon* **1970**, *6*, 1.
(9) Crowell, A.; Young, D. *Trans. Faraday Soc.* **1953**, *49*, 1080.
(10) Crowell, A. *J. Chem. Phys*. **1957**, *26*, 1407.
(11) Crowell, A.; Steele, W. A. *J. Chem. Phys.* **1961**, *34*, 1347.
(12) Gardner, L.; Kruk, M.; Jaroniec, M. *J. Phys. Chem. B* **2001**, *105*, 12516.
(13) Blumel, S.; Koster, F.; Finedenegg, G. *J. Chem. Soc., Faraday Trans.* **1982**, *78*, 1753.
(14) Findenegg, G. *J. Chem. Phys.* **1984**, *81*, 3270.
(15) Glanz, P.; Findenegg, G. *Adsorpt.: Sci. Tech*. **1984**, *1*, 41.
(16) Specovius, J.; Findenegg, G. *Ber. Bunsen-Ges. Phys. Chem*. **1978**, *82*, 174.
(17) Graham, D. *J. Phys. Chem*. **1957**, *61*, 1310.
(18) Graham, D. *J. Phys. Chem*. **1962**, *66*, 1815.
(19) Norman, G. E.; Filinov, V. S. *High Temp. (USSR)* **1969**, *7*, 216.
(20) Frenkel, D.; Smit, B. *Understanding Molecular Simulation*; Academic Press: New York, 2002.
(21) Steele, W. A. *Surf. Sci. Ser.* **1999**, *78*, 319.

10.1021/la052545i CCC: $33.50
Published on Web 12/27/2005

shape is very important in the structure of the adsorbed phase and the packing density. Rather, we should consider it to be a particle composed of at least six interaction sites to model the molecular shape properly. We write below the interaction energy between a site *a* on a molecule *i* with a site *b* on a molecule *j* using a Lennard-Jones 12-6 equation:

$$\varphi_{i,j}^{(a,b)} = 4\epsilon^{(a,b)}\left[\left(\frac{\sigma^{(a,b)}}{r_{i,j}^{(a,b)}}\right)^{12} - \left(\frac{\sigma^{(a,b)}}{r_{i,j}^{(a,b)}}\right)^{6}\right] \quad (1)$$

The subscript is used for a particle, and the superscript is used for a site. Thus, for a given intersite distance $r_{i,j}^{(a,b)}$, to calculate the interaction energy $\varphi_{i,j}^{(a,b)}$ we need to know the cross collision diameter $\sigma^{(a,b)}$ and the cross well depth of the interaction energy $\epsilon^{(a,b)}$. They can be determined by invoking the mixing rule due to Lorentz−Berthelot (LB), $\sigma^{(a,b)} = [\sigma^{(a,a)} + \sigma^{(b,b)}]/2$ and $\epsilon^{(a,b)} = \sqrt{\epsilon^{(a,a)}\epsilon^{(b,b)}}$. Knowing the site−site interaction, the interaction between two molecules is simply (assuming pairwise additivity) $\varphi_{i,j} = \sum_{a=1}^{M}\sum_{b=1}^{M}\varphi_{i,j}^{(a,b)}$, where M is the number of sites on each molecule. (M ranges from 6 to 12, depending on the model used.)

We have just addressed the interaction energy between two molecules where the interaction is due to dispersive forces. Although benzene has a zero dipole, it has a reasonably high quadrupole moment (-23.9×10^{-40} C m^{-2}). The quadrupole moment can be accounted for in the total intermolecular interaction by specifying a set of discrete partial charges and their locations. Knowing this information, the interaction between a charge on one molecule with a charge on another molecule can be carried out exactly the same way as done with dispersive interaction sites above. The interaction energy due to the electrostatic force between a charge α on a molecule *i* and a charge β on a molecule *j* is determined via the Coulomb law of electrostatic interaction[22]

$$\varphi_{q;i,j}^{(\alpha,\beta)} = \frac{1}{4\pi\epsilon_0}\frac{q_i^{\alpha}\, q_j^{\beta}}{r_{i,j}^{(\alpha,\beta)}} \quad (2)$$

where ϵ_0 is the permittivity of free space [$\epsilon_0 = 10^7/(4\pi c^2) = 8.8543 \times 10^{-12}$ C^2 J^{-1}m^{-1}, c is the speed of light], $r_{i,j}^{(\alpha,\beta)}$ is the distance between two charges α and β on molecules *i* and *j*, respectively, q_i^{α} is the value of charge α on molecule *i*, and q_j^{β} is the value of charge β on molecule *j*. The electrostatic interaction between two molecules takes the form $\varphi_{q;i,j} = \sum_{\alpha=1}^{M_q}\sum_{\beta=1}^{M_q}\varphi_{q;i,j}^{(\alpha,\beta)}$. Here, M_q is the number of charges on the molecule. For benzene, the number of charges is either 3 or 12 for the two models considered in this article.

For the characterization of activated carbon having small pores, benzene is often used because of the well-known slit shape of micropores and the flat shape of the benzene molecule. The popularity of benzene in the characterization of activated carbon is reflected in its use as the reference probe in the evaluation of the characteristic energy in the well-known Dubinin−Raduskevitch (DR) and Dubinin−Astakhov (DA) equations.[23,24] Although it is well used in the area of characterization, an understanding of benzene adsorption on graphite is not well supported by molecular simulation tools, especially because of the lack of credible potential models to describe the adsorption isotherm correctly.

Table 2. Parameters of the Two Models of Jorgensen et al.[26] and Wick et al.[27]

parameter	OPLS	TraPPE
σ (A)	3.75	3.695
ϵ/k (K)	55.3	50.5

Table 3. Parameters of the Jorgensen and Severance Model for Benzene[2]

parameter	σ (A)	ϵ/k (K)	q (e)
C atom	3.550	35.22733	−0.115
H atom	2.420	15.09743	+0.115

There are a number of intermolecular potential models for benzene that have been proposed in the literature. A review of older models has been given in Vernov and Steele.[25] We will consider four models that have recently been proposed in the literature. The first two models that we consider were proposed by Jorgensen et al. (OPLS)[26] and Wick et al. (TraPPE).[27] Both of them belong to the general class of the united atom model. They have six dispersive sites, which coincide with the centers of six carbon atoms. The C−C bond length in both of these models is 1.4 Å. The parameters of these two models are listed in Table 2. These two models are similar, and because the TraPPE model has been tested for its performance against vapor−liquid equilibria (VLE), we believe that a good prediction of VLE is a prerequisite for adsorption studies.[28−32] Therefore, we shall consider the TraPPE model in this investigation to represent models with only dispersive forces.

The next two models are those accounting for electrostatic interaction explicitly. This is done by the specification of a set of discrete partial charges. One of those models is the modification from an earlier model of Wick et al.,[27] accounting for a set of discrete partial charges to reproduce the quadrupole moment.[1] There are six dispersive sites that lie at the centers of the carbon atoms. The C−C bond length is 1.4 Å, and the molecular parameters for these sites are $\sigma = 3.74$ Å and $\epsilon/k = 48$ K. Because this model explicitly accounts for the electrostatic effect, the well depth for the fluid−fluid interaction is less than that of the TraPPE model. To account for the quadrupole moment, a positive partial charge (2.42 e) is put at the center of the benzene ring, and two negative partial charges (−1.41 e) are placed at a distance of 0.785 Å on both sides of the ring along the line perpendicular to the ring. We denote this model as WSKS to stand for the initials of the authors of Wick et al.'s paper.[1]

The last model is that by Jorgensen and Severance (JS)[2], and it is an all-atom model. It contains 12 dispersive sites and 12 partial charges at the centers of carbon and hydrogen atoms. The molecular parameters and the partial charges are listed in Table 3. The C−C and C−H bond lengths are 1.40 and 1.08 Å, respectively. Because this model contains 12 dispersive sites and 12 charge sites, the number of calculations of the intermolecular interaction energy is 144 (because the 12 partial charges reside at the same locations as those dispersive sites), compared to 45 in the WSKS model. As a result, the JS model requires at least 1 order of magnitude of computation time, compared to the WSKS model.

(22) Tipler, P. *Physics*; Freeman and Company/Worth Publishers: New York, 1999.
(23) Do, D. D. *Adsorption Analysis: Equilibria and Kinetics*; Imperial College Press: London, 1998.
(24) Rudzinski, W.; Everett, D. *Adsorption of Gases on Heterogeneous Surfaces*; Academic Press: New York, 1992.
(25) Vernov, A.; Steele, W. *Langmuir* **1991**, *7*, 2817, 3110.
(26) Jorgensen, W. L.; Madura, J. D.; Swenson, C. J. *J. Am. Chem. Soc.* **1984**, *106*, 6638.
(27) Wick, C. D.; Martin, M. G.; Siepmann, J. I. *J. Phys. Chem. B* **2000**, *104*, 8008.
(28) Do, D. D.; Do, H. D.; Kaneko, K. *Langmuir* **2004**, *20*, 7623.
(29) Do, D. D.; Do, H. D. *Adsorpt. Sci. Technol.* **2005**, *23*, 267.
(30) Do, D. D.; Do, H. D. *Fluid Phase Equilib.* **2005**, *236*, 169.
(31) Do, D. D.; Do, H. D. *Mol. Simul.* **2005**, *31*, 651.
(32) Do, D. D.; Do, H. D. *J. Colloid Interface Sci.* **2005**, *287*, 432.

Method of Calculating the Electrostatic Interaction in a Simulation Box. The interaction energy by electrostatic interaction of charge α is calculated by summing the interactions between charge α and other charges β in the simulation box and charge α with all charges in the image boxes (including its own image). Let n_C be the number of images (in the *x* and *y* directions; *z* is the direction normal to the pore surface) for which the calculation of interaction energy is performed. To calculate the long-range correction from images $n_C + 1$ onward, we use the approach of Heyes and van Swol.[33] The interaction energy of charge α is

$$\varphi_q^{(\alpha)} = \frac{1}{2}\sum_{\beta=1}^{N} \frac{q^{(\alpha)}q^{(\beta)}}{4\pi\epsilon_0}\left[\sum_{|n_x|=0}^{n_C}\sum_{|n_y|=0}^{n_C}{}' \frac{1}{|\underline{r}^{(\alpha,\beta)} + n_xL + n_yL|} + \frac{\pi}{n_CL^3}\{[x^{(\alpha,\beta)}]^2 + [y^{(\alpha,\beta)}]^2 - 2[z^{(\alpha,\beta)}]^2\}\right] \quad (3)$$

where *L* is the box length and $x^{(\alpha,\beta)}$, $y^{(\alpha,\beta)}$, and $z^{(\alpha,\beta)}$ are the distances between charges α and β in the *x*, *y*, and *z* directions, respectively.

Solid−Fluid Potential. For a polyatomic molecule with *M* LJ-type centers, the solid−fluid interaction energy can be determined as follows. The interaction potential energy between site *a* of molecule *i* and the homogeneous flat solid substrate is calculated by the 10-4-3 Steele potential.[34−35] It takes the following form

$$\varphi_{i,s}^{(a)} = 4\pi\rho_C\epsilon^{(a,s)}[\sigma^{(a,s)}]^2\Delta\left\{\frac{1}{5}\left(\frac{\sigma^{(a,s)}}{z_i^a}\right)^{10} - \frac{1}{2}\left(\frac{\sigma^{(a,s)}}{z_i^a}\right)^4 - \frac{[\sigma^{(a,s)}]^4}{6\Delta(0.61\Delta + z_i^a)^3}\right\} \quad (4)$$

where ρ_c is the volumetric carbon atom density (114 nm^{-3}) and Δ is the spacing between the two adjacent graphite layers (0.3354 nm). The solid−fluid molecular parameters, the collision diameter $\sigma^{(a,s)}$, and the interaction energy $\epsilon^{(a,s)}$ are calculated from the Lorentz−Berthelot mixing rule. The solid−fluid interaction energy is usually adjusted with the introduction of the solid−fluid binary interaction parameter k_{sf} such that the experimental Henry's constant is reproduced by the GCMC simulations, that is, $\epsilon^{(a,s)} = (1 - k_{sf})\sqrt{\epsilon^{(a,a)}\epsilon^{(s,s)}}$. Here we assume that the binary interaction parameter k_{sf} is the same for all interaction sites of a molecule. Having the interaction potential energy of site *a* of molecule *i* with the surface as given in eq 4, the solid−fluid interaction energy of molecule *i* is simply $\varphi_{i,s} = \sum_{a=1}^{M}\varphi_{i,s}^{(a)}$.

3. Results and Discussion

In the GCMC simulations of adsorption on graphitized thermal carbon black, we use the following parameters. Generally, the box length is 10 times the collision diameter, and the cutoff radius is taken to be half of the box length. The number of cycles in the equilibration step and in the collecting statistics step is 50 000 each. In each cycle we have *N* displacements and *N* rotations (*N* is the number of particles), and the number of attempt to exchange particles with the surroundings is chosen as 2*N*. The type of move is chosen randomly in the simulation to ensure microscopic reversibility. In presenting the results, we plot them as (i) surface excess versus pressure (isotherm), (ii) a 2D plot of local density versus the distance above the surface, and (iii) a 3D plot of local density versus the distance above the surface and the angle formed between the molecular axis and the *z* direction (perpendicular to the pore surface). The average surface excess is defined as

$$\Gamma_{av} = \frac{\langle N\rangle}{L_xL_y} - \frac{\rho L_xL_yH'}{L_xL_y} \quad (5)$$

where ρ is the bulk molecular density, L_x and L_y are the box lengths in the *x* and *y* directions, respectively, $\langle N\rangle$ is the ensemble average of the number of particles in the pore, and H' is the accessible pore width. The latter is defined as the width that is accessible to a benzene molecule. This is done as follows. The volume space that is accessible to the center of mass (COM) of a particle is defined as the space in which the solid−fluid potential energy is less than zero. This is done in a similar way to that of Kaneko et al.,[36] who dealt with 1C-LJ particle. Thus if we define z_0 as the distance from the carbon surface at which the solid−fluid potential energy is zero, then the accessible pore width is (assuming benzene is parallel to the carbon surface)

$$H' = H - 2z_0 + \sigma^{(C,C)} \quad (6)$$

where *H* is called the physical pore width. We use a pore of width 80 Å in our simulation to mimic two independent surfaces, and for this width, the distance z_0 is 3.0327 Å and the accessible pore width is 77.6746 Å.

The local density is defined as $\rho(z) = \langle DN(z)\rangle/L_xL_y\Delta z$, where $\Delta N(z)$ is the number of molecules whose centers of mass are located in the segment having boundaries at *z* and $z + \Delta z$ and L_x and L_y are the box lengths in the *x* and *y* directions, respectively. In the 3D plot of the local density distribution, it is calculated from[37] $\rho(z, \theta) = \langle DN(z, \theta)\rangle/L_xL_y\Delta z \sin\theta\,\Delta\theta$, where $\Delta N(z, \theta)$ is the number of benzene molecules whose centers of mass are located in the segment having boundaries *z* and $z + \Delta z$ and the angle between the normal of the benzene ring and the *z* direction falls between θ and $\theta + \Delta\theta$. This plot of $\rho(z, \theta)$ versus *z* and θ allows us to evaluate the preferential orientation of the molecules located various distances from the wall surface. An angle of 0 means that the molecule lies parallel to the pore wall, and a value of $\pi/2$ means that the molecule is perpendicular to the pore surface.

A thermodynamic quantity of interest that can be readily obtained from the GCMC is the isosteric heat. Using the fluctuation theory,[38] the isosteric heat is calculated from[39]

$$q_{iso} = \frac{\langle U\rangle\langle N\rangle - \langle UN\rangle}{\langle N^2\rangle - \langle N\rangle\langle N\rangle} + kT \quad (7)$$

where $\langle\ \rangle$ is the ensemble average, *N* is the number of particles, and *U* is the configuration energy of the system. This configuration energy can be divided into two contributions: one is due to the fluid−fluid interaction, and the other is due to the fluid−solid

(33) Heyes, D. M.; van Swol, F. *J. Chem. Phys.* **1981**, *75*, 5051.
(34) Steele, W. A. *Surf. Sci.* **1973**, *36*, 317.
(35) Steele, W. A. *The Interaction of Gases with Solid Surfaces*; The International Encyclopedia of Physical Chemistry and Chemical Physics; Pergamon Press: Oxford, U.K., 1974; Topic 14, Vol. 3.
(36) Kaneko, K.; Cracknell, R.; Nicholson, D. *Langmuir* **1994**, *10*, 4606.
(37) Klochko, A.; Brodskaya, E. N.; Piotrovskaya, E. M. *Langmuir* **1999**, *15*, 545.
(38) Hill, T. *Statistical Mechanics*; Dover: New York, 1956.
(39) Nicholson, D.; Parsonage, N. *Computer Simulation and the Statistical Mechanics of Adsorption*; Academic Press: London, 1982.

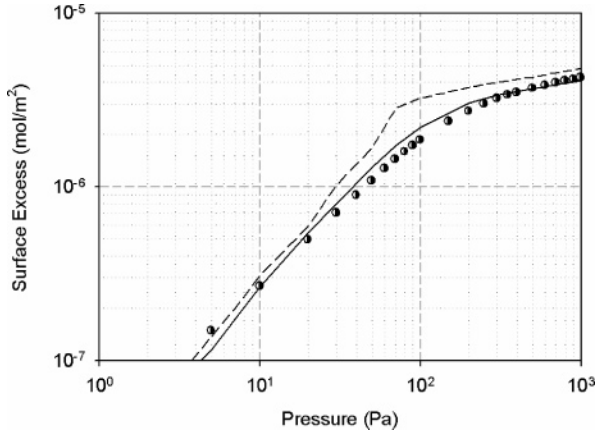

Figure 1. Adsorption isotherm of benzene on graphitized thermal carbon black at 293 K. Filled symbols, data of Isirikyan and Kiselev;[3] dashed line, original model of WSKS; solid line, modified WSKS model with surface mediation.

interaction, that is, $U = U_{ff} + U_{sf}$:

$$q_{iso} = \left[\frac{\langle U_{ff}\rangle\langle N\rangle - \langle U_{ff}N\rangle}{\langle N^2\rangle - \langle N\rangle\langle N\rangle} + kT\right] + \frac{\langle U_{sf}\rangle\langle N\rangle - \langle U_{sf}N\rangle}{\langle N^2\rangle - \langle N\rangle\langle N\rangle} \quad (8)$$

The square bracket term in the RHS of the above equation is the contribution from the fluid−fluid interaction and the molecular thermal energy, whereas the remaining term is the contribution from the interaction between fluid and solid.

Benzene Adsorption on GTCB. Experimental data of benzene on graphite or graphitized thermal carbon black are available from Isirikyan and Kiselev[3] at 293 K, whereas wider temperature range data are available from Pierotti and Smallwood[4] and Belyakova, Kiselev, and Kovaleva.[6] Limited data are available from Pierce and Ewing[5] and Carrott et al.,[7] but in this work, we will restrict ourselves to the more extensive data of Isirikyan and Kiselev, Pierotti and Smallwood, and Belyakova et al.

Data of Isirikyan and Kiselev.[3] This set of data, published in 1961, is the first comprehensive data of benzene on graphitized thermal carbon black at 293 K. Adsorption isotherm and isosteric heat data are available, and it makes this set very suitable for testing the intermolecular potential models for benzene. First, we test the WSKS model of Wick et al.,[1] which is known to reproduce VLE with high accuracy. It is worthwhile to point out here is that the molecular parameters of the original WSKS model were obtained from the fit between the simulation results and the vapor−liquid equilibria data, and the truncation of 1.4 nm was used in the calculations of both dispersion and quadrupolar interactions. We used here a cutoff radius ranging from 1.3 to 1.8 nm and have found that the effect of using a different cutoff radius is negligible. Furthermore, we also explore the difference in the truncation cutoff and the Heyes and van Swol 2D long-range data for electrostatic interaction and found that it is small.

First, we apply the original WSKS (without surface mediation) in the GCMC simulation of benzene adsorption on graphite. The results are shown in Figure 1 as a dashed line, and the experimental data, as filled symbols. By studying the simulation results against the experimental data in this Figure, we see that the GCMC simulation results show a distinct upward bend in the region where the first layer is being completed, reaching a plateau of about 4 μmol/m^2. Given the molecular projection area of benzene[3] as 40 Å^2, the surface density of 4 μmol/m^2 corresponds to complete monolayer coverage.

Although the simulation results show a distinct sharp upward bend in the region of monolayer completion, the experimental data clearly do not. This suggests that the fluid−fluid interaction in the adsorbed phase is overestimated by the model. The graphite surface exerts an influence on the behavior of the adsorbed molecules close to the surface. We argue that this surface mediation has the effect that the fluid−fluid interaction of the adsorbed molecule is less than that of the free molecule (which means that the quadrupole moments of adsorbed benzene are less than that of free molecules). To test this, we introduce an empirical way to reduce the fluid−fluid interaction by reducing the contribution of each benzene molecule in the intermolecular fluid−fluid interaction by a factor F whenever that molecule is in the first layer. With this implemented in the GCMC simulation, we have found that the simulation results agree well with the experimental data when F is equal to 0.9 (solid line in Figure 1). What this means is that the dispersive contribution is reduced by 10% and the quadrupole moment is also reduced by the same amount. Thus, surface mediation is important, and this leads to the reduction of the fluid−fluid interaction.

Before we consider the microscopic pictures of adsorption, we need to further test the hypothesis of surface mediation on the reduction of fluid−fluid interaction between adsorbed molecules. We do this by testing the isosteric heat obtained from the GCMC simulation and comparing it with the data obtained by Isirikyan and Kiselev.[3] In this work, they studied the adsorption of nitrogen at 77 K, that of *n*-hexane at 293 K, and that of benzene at 293 K on the same graphitized thermal carbon black. The isosteric heat for nitrogen and *n*-hexane exhibits a linear increase with loading in the submonolayer region, and this is attributed to the adsorbate−adsorbate interaction. However, the experimental isosteric heat of benzene adsorption on GTCB exhibits a different pattern; it is more or less constant in the submonolayer region. The explanation for this pattern is that the linear increase in heat due to the adsorbate−adsorbate interaction is more or less compensated for by the linear decrease in heat due to the solid−fluid interaction. The latter is the case because as loading is increased in the submonolayer region some benzene molecules orient themselves with a slant configuration against the graphite surface to maximize the quadrupolar interaction. As a result, their centers of mass are further away from the surface, and the solid−fluid interaction is decreased as a result. This then gives rise to the linear decrease in the heat contributed by solid−fluid interaction. By pure coincidence, this linear decrease in the heat contributed by solid−fluid interaction is more or less compensated for by the linear increase in the heat contributed by fluid−fluid interaction.

Figure 2 shows the isosteric heat versus loading. Experimental data of Isirikyan and Kiselev[3] are shown as symbols, and the GCMC simulation results of using the original WSKS model (i.e., without surface mediation) are shown in this Figure as the dashed line. We see that the original WSKS model shows a significant increase in the isosteric heat versus loading in the submonolayer region, and this is a consequence of the overprediction of the adsorbate−adsorbate interaction by the original model of Wick et al.[1] In the modified intermolecular potential model in which we reduce the fluid−fluid interaction of each molecule by a factor of $F = 0.9$ whenever that molecule is in the first layer, the GCMC simulation results of isosteric heat are shown as the solid line. Now we see that the GCMC simulation results, using the modified potential model, agree extremely well with the experimental data; that is, they indeed predict the constant isosteric heat in the submonolayer coverage region. To see the contributions of the solid−fluid and fluid−fluid interactions, we

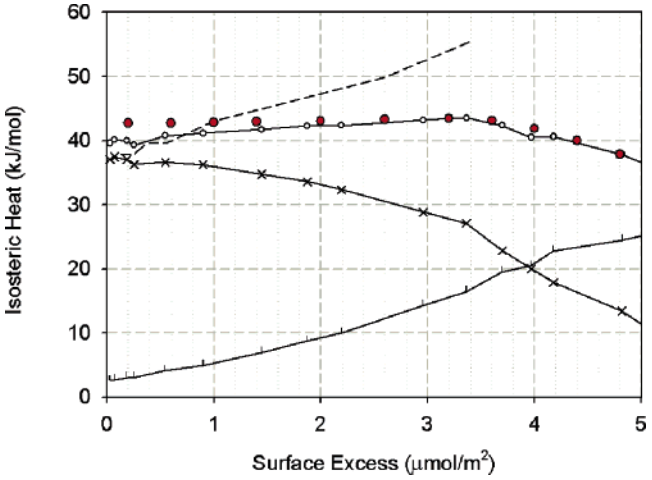

Figure 2. Isosteric heat vs loading for benzene adsorption on GTCB at 293 K using the WSKS model. Filled symbols are the experimental data of Isirikyan and Kiselev, and the solid line with circle symbols is the GCMC results using the WSKS with surface mediation. The solid line with cross symbols is the contribution of the solid−fluid interaction to the isosteric heat, and the solid line with vertical bars is the contribution of the fluid−fluid interaction.

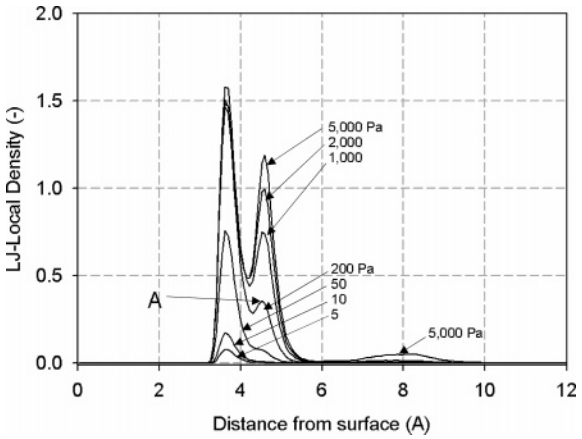

Figure 3. Local density distribution vs distance from the graphite surface at 293 K using the WSKS model for $P = 5$, 10, 50, 200, 1000, 2000, and 5000 Pa.

also plot in Figure 2 the heats that are contributed by these interactions. It is now clearly seen that the heat contributed by the solid−fluid interaction (solid line with cross symbols) decreases with loading in the submonolayer coverage region and that it is more or less compensated for by the increase in heat contributed by the fluid−fluid interaction (solid line with bar symbols).

To support the decrease in heat contributed by solid−fluid interaction, we investigate the local density distribution of benzene versus the distance from the surface of one pore wall and the angle θ formed by the normal vector of the benzene ring and the z axis normal to the graphite surface. First we consider the local density distribution versus distance for a number of pressures (5, 10, 50, 200, 1000, 2000, and 5000 Pa) as shown in Figure 3. In this Figure, we see that the first layer is about 3.5 Å from the surface and the second layer is about 7.5 Å from the surface and starts to form at a pressure of about 1000 Pa. At low pressures, benzene molecules adopt the parallel orientation, and when the pressure is about 200 Pa, we observe the appearance of a shoulder evolving from the first peak about 4.5 Å from the graphite surface (point A in Figure 3). This shoulder is due to a small portion of benzene molecules in the first layer changing from the parallel orientation to the slant or vertical orientation. When pressure is increased to 1000 Pa, we see that the second layer is formed 7.5 Å from the surface and the portion of benzene molecules in the first layers taking the slant or vertical orientation is increased as seen in the evolution of shoulder A into a distinct peak at 4.5 Å. The reason for the greater portion of benzene molecules taking the slant orientation in the first layer is the presence of the second layer, whose intermolecular interaction with those in the first layer will cause some in the first layer to take orientations other than the parallel orientation. Thus, the first layer has two overlapped peaks, one at 3.5 Å and the other at 4.5 Å. They correspond to particles adopting parallel and slant orientations, respectively. Knowing the carbon−carbon length of the WSKS model to be 1.4 Å, we can calculate the angle of the benzene molecule corresponding to the peak at 4.5 Å to be about 45°.

As pressure is increased further beyond 1000 Pa, we see that more and more benzene molecules in the first layer adopt the 45° slant orientation, as seen in the increase in intensity of the 4.5 Å peak. It is because of the 45° slant orientation of some benzene molecules in the first layer that their centers of mass are further away from the surface. This leads to a reduction in the heat contributed by the solid−fluid interaction. (See the solid line with cross symbols in Figure 2.) This reduction in the heat contributed by the solid−fluid interaction is then compensated for by an increase in the heat contributed by the fluid−fluid interaction, resulting in a reasonably constant heat over the region of monolayer coverage (0−4 μmol/m^2).

To see further the orientation of benzene in various layers, we present the 3D plot of the local density distribution versus the distance from the surface and the angle θ in Figure 4. We see that at very low loading (Figure 4a) benzene molecules lie flat on the surface as seen in Figure 4a, with most benzene molecules taking an angle θ of 0. (θ is defined as the angle between the normal vector of the benzene ring and the vertical z axis of the surface.) This parallel orientation at low loading is due to the fact that this is the most favorably energetic position. When the loading is increased but still within the submonolayer coverage, the closeness of adsorbed molecules will result in stronger fluid−fluid interaction via both dispersive and electrostatic interactions. To maximize the quadrupolar interaction, benzene molecules will orient themselves such that some molecules will adopt slant configurations while the others remain horizontal along the pore walls as seen in Figure 4b. In this Figure, we see that the first layer has molecules at a distance of 3.5 Å having an angle of zero, meaning that they have parallel orientation, and it also has molecules adopting an angle greater than zero. That is, there are molecules taking a slant or vertical orientation. It is this slant configuration that results in decreased heat due to the solid−fluid interaction.

The snapshot of Figure 5 shows the orientation of benzene molecules at 300 and 2000 Pa. We see that most benzene molecules in the submonolayer coverage (300 Pa) adopt the parallel orientation while a much smaller population adopts the slant orientation. This is to maximize the quadrupolar interactions, and this is further substantiated with a snapshot at 2000 Pa, where we see that a greater portion takes the vertical orientation.

Next we study the performance of the other two intermolecular potential models. First, let us consider the TraPPE model of Wick et al.,[27] which considers only dispersive forces. The contribution of the Coulombic forces is embedded in the effective molecular parameters. We show in Figure 6 the performance of this model, with Figure 6a showing the comparison between the GCMC-simulated isotherm and the experimental data and Figure

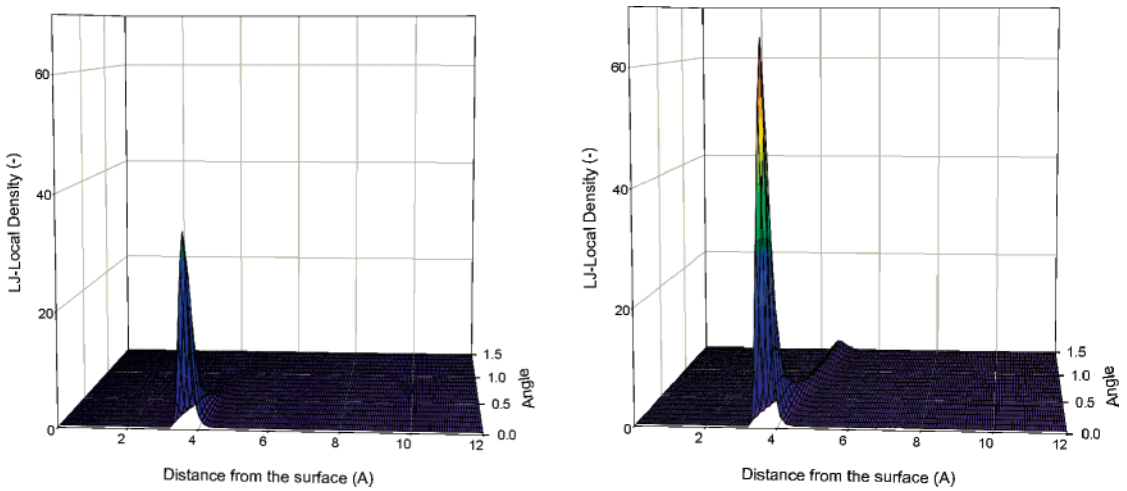

Figure 4. Three-dimensional local density distribution vs distance from the surface and the angle between the normal vector of the benzene ring and the z axis normal to the graphite surface. (Left) $P = 50$ Pa (low loading); (right) $P = 2000$ Pa (high loading).

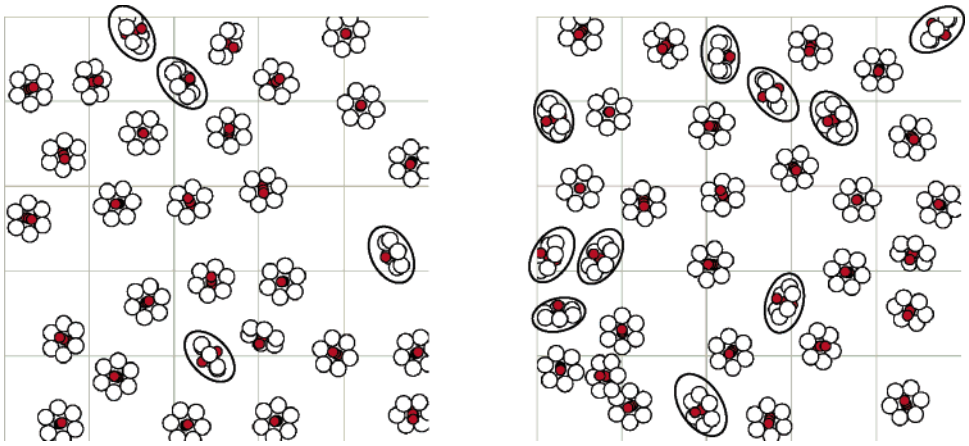

Figure 5. Top view of the snapshot of benzene molecules (not to scale for clarity) on the graphite surface at 293 K. (Left) 300 Pa; (right) 2000 Pa.

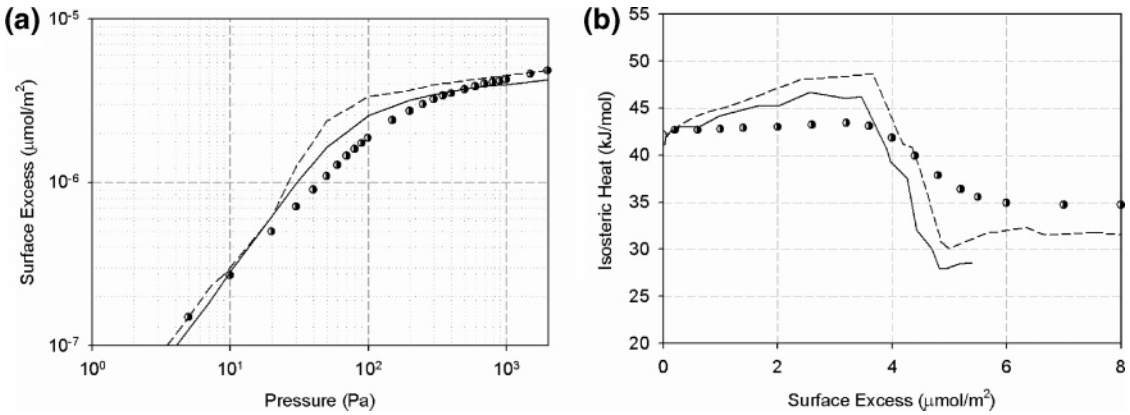

Figure 6. Adsorption isotherm and isosteric heat obtained from the TRaPPE model. Symbols, data of Isirikyan and Kiselev; dashed line, GCMC simulation results without surface mediation; solid line, GCMC results with surface mediation.

6b presenting the corresponding isosteric heats versus loading. The dashed line is the simulation result without accounting for the surface mediation, whereas the solid line is that with surface mediation. It is seen that this model is not adequate for the description of the adsorption isotherm and the isosteric heat, although the correlation of the adsorption isotherm data might be regarded as acceptable.

The TraPPE model predicts an increase in the isosteric heat in the submonolayer coverage, which is in contrast to the constant experimental heat in this region. Finally, we consider the last model, JS, which is the most comprehensive model. It contains 12 dispersive sites and 12 partial charges; therefore, its requirement of computation time is extremely large, usually 1 order of magnitude longer than for the the WSKS and TraPPE models. Figure 7 shows the plots of the surface excess versus pressure and the isosteric heat versus loading. We see that this model reasonably describes the experimental isotherm data but poorly describes the isosteric heat versus loading in the region of submonolayer coverage. Thus, we can conclude that the WSKS is the best model for the prediction of the adsorption isotherm

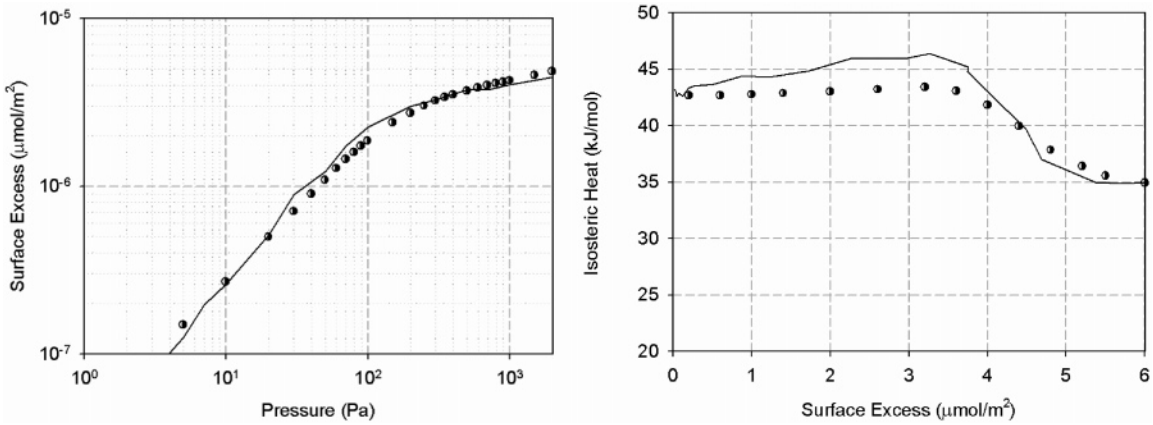

Figure 7. Adsorption isotherm (left) and isosteric heat (right) obtained from the JS model. Symbols, experimental data of Isirikyan and Kiselev; solid line, GCMC simulation results.

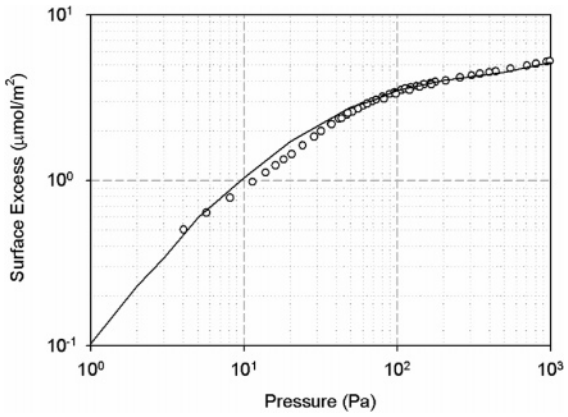

Figure 8. Adsorption isotherm of benzene on GTCB at 273 K (data of Pierotti and Smallwood).

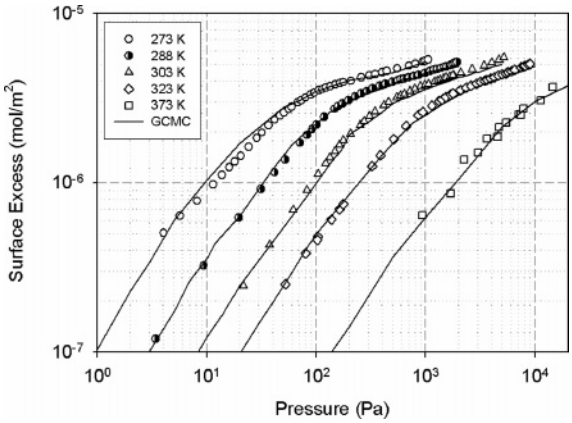

Figure 9. Adsorption isotherms of benzene on GTCB at 273, 288, 303, 323, and 373 K (data of Pierotti and Smallwood and Belyakova et al.).

as well as the isosteric heat. Despite its complexity and the longer computation time involved, the JS model does not perform as well.

Data of Pierotti and Smallwood[4] and Belyakova et al. Because the WSKS model has shown its superiority in terms of prediction as well computation time, we will check its performance against data at other temperatures. We do this with Pierotti and Smallwood's data[4] at 273, 288, 303, 323, and 373 K, and Belyakova et al.'s data[6] at 303 and 323 K. These authors produced the most comprehensive data for benzene on GTCB, and this is a further test of the performance of the WSKS model.

First, we test with the lowest temperature, 273 K, which is below the triple point of benzene. Figure 8 shows the adsorption isotherms with symbols representing the data and the solid line from the GCMC simulations. The simulation results (solid line) are obtained with the WSKS model and the allowance for surface mediation. To get good agreement between the simulation results and the data, we find that the reduction factor F is 0.9, which is exactly the same as that obtained for the data of Isirikyan and Kiselev at 293 K. To show the importance of surface mediation, we also show in Figure 8 the simulation results when surface mediation is absent (dashed line).

We consider the data of Pierotti and Smallwood at higher temperatures (288, 303, 323, and 373 K) and that of Belyakova et al., and the results for the adsorption isotherm are shown in Figure 9. As seen in this Figure, the adsorption isotherms at various temperatures are reasonably correlated by the WSKS potential model.

We finally show the temperature dependence of the isosteric heat, and this is shown in Figure 10 for 293 and 343 K. We see

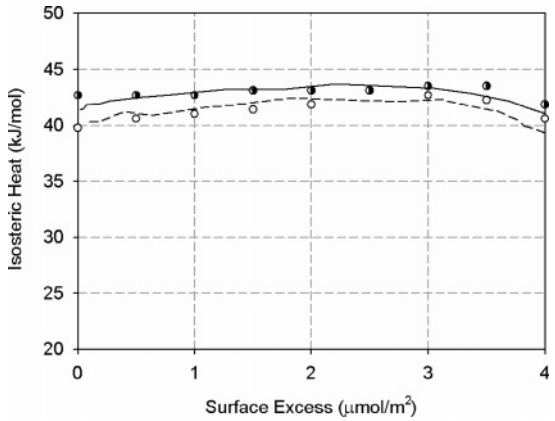

Figure 10. Isosteric heat of benzene on GTCB at 293 and 343 K. Data of Avgul and Kiselev. Unfilled circles, 343 K data; half-filled symbols, 293 K data; solid line, GCMC results at 293 K using the modified WSKS model with surface mediation; dashed line, GCMC results at 343 K using the modified WSKS model with surface mediation.

that there is a weak temperature dependence of the isosteric heat. The isosteric heat decreases with temperature for a given loading as one would expect physically.

4. Conclusions

We have presented in this article a simulation study of benzene adsorption on graphitized thermal carbon black. Surface mediation is important in the correct description of benzene adsorption on

GTCB. We tested this with a number of data in the literature, and we concluded that the correct choice of model is important, that the quadrupolar effect must be explicitly accounted for to explain the behavior of isosteric heat versus loading, and that surface mediation also must be accounted for. Among the models tested, the WSKS is the most appropriate model in the description of benzene adsorption, and surface mediation is quantified by reducing the contribution of each molecule to the fluid−fluid interaction by 10% whenever that molecule is in the first layer close to the surface.

Acknowledgment. This work is supported by the Australian Research Council.

LA052545I